

Topological Acoustic Diode

Ashwat Jain,^{1,*} Wojciech J. Jankowski,^{2,†} M. Mehraeen,^{1,‡} and Robert-Jan Slager^{1,2,§}

¹*Department of Physics and Astronomy, University of Manchester, Oxford Road, Manchester M13 9PL, UK*

²*Theory of Condensed Matter Group, Cavendish Laboratory, University of Cambridge, J. J. Thomson Avenue, Cambridge CB3 0HE, UK*

(Dated: January 30, 2026)

We show that certain three-dimensional topological phases can act as acoustic diodes realizing nonlinear odd acoustoelastic effects. Beyond uncovering topologically-induced anomalous acoustic second-harmonic generation and rectification, we demonstrate how such nonlinear responses are uniquely captured by the momentum-space nonmetricity tensor in the quantum state Hilbert-space geometry. In addition to completing the classification of quantum geometric observables in the quadratic response regime, our findings reveal unexplored avenues for experimental realizations of acoustic diodes using effective θ vacua of axion insulators adaptable for topological engineering applications.

Introduction.—Nonlinear phenomena constitute a growing field of interest, underpinned by various theoretical and experimental advances [1–8]. Fundamentally, these effects arise from anharmonicities in various forms of matter subject to time-dependent forcing, which can notably culminate in second-harmonic generation (SHG), manifested by a frequency doubling in responses [9]. Among such nonlinear effects, of particular technological interest are rectifications, that is conversions of ac currents to dc currents, which are definitional to the operating principle of diodes. Although such phenomena in matter typically arise as a response to electromagnetic stimulation, similar nonlinear responses can also arise upon perturbing crystals with acoustic waves, or sound [10, 11]. Recent advances within this scope involve acoustoelectric effects, such as quantum nonlinear acoustic Hall effects [12].

Experimentally accessible and fundamentally intriguing topological materials [13–22] are particularly promising for realizing unconventional nonlinear effects. Exotic nonlinearities in responses of topological matter can be captured by current correlators, where intrinsic effects arise at the level of one-loop diagrams via propagators of topological quasiparticles and their coupling to external forcing fields, represented by vertices [23–26]. In that context, electromagnetic nonlinearities, including optical responses and magnetoresistances, are naturally supported by three-dimensional topological insulators [13, 27–30], such as axion insulators [31, 32], and topological semimetals such as Weyl and Dirac materials [20, 33–37]. In particular, nonlinear optical responses manifested as rectified currents culminate in topological bulk photovoltaic effects [38], such as quantized circular photogalvanic effects due to Berry curvature [39], or shift responses due to Hermitian connections [40, 41] and band torsion [42]. Formally, exotic nonlinear responses may be

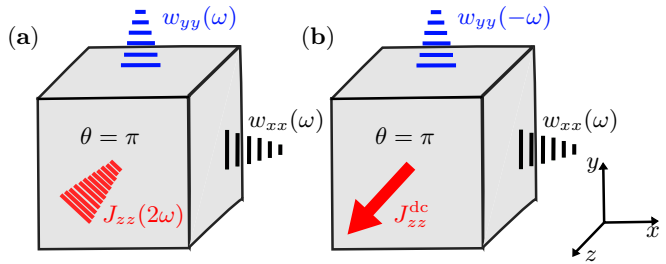


FIG. 1. Topological acoustic diode responses. **(a)** Odd acoustic second-harmonic generation. **(b)** Odd acoustic rectification. The nonlinear acoustic responses to time-dependent distortion fields $w_{ij}(\omega)$ are topologically-induced by the θ -vacuum of an axion insulator ($\theta = \pi$). The acoustoelastic frequency-doubling $J_{zz}(2\omega)$ and rectified J_{zz}^{dc} currents flow in the z direction, orthogonally to the mutually perpendicular forcing directions (x, y).

phrased in terms of broader classes of quantum geometric tensors (QGTs) [8, 26, 40, 41, 43, 44], demonstrating a deeper interplay of momentum-space Riemannian geometry and quantum response theory [41]. While the original formulations of quantum geometric quantities date back to the last century [45], their physical manifestations beyond correlated [46] or optical phenomena [41, 47] have initiated several current research directions [8, 48].

Moving beyond the domain of electromagnetic responses, QGTs have recently been shown to manifest in nonlinear viscoelastic phenomena [49]. Notably, such nonlinear elastic responses involve unique geometric structures in the parameter spaces of deformation fields, rather than single-particle momenta [49–51]. Such non-trivial quantum geometries can be induced by topological invariants, although the according viscoelastic effects go beyond the strict presence of topology. In particular, these effects persist upon breaking the symmetries protecting the nontrivial topologies. Elastic nonlinearities can therefore galvanize uncharted avenues for further exploration of quantum responses that are driven by unprecedented gauge-invariant, and thus measurable, geometric tensor quantities.

* ashwat.jain@postgrad.manchester.ac.uk

† wjj25@cam.ac.uk

‡ mandela.mehraeen@manchester.ac.uk

§ robert-jan.slager@manchester.ac.uk

In this work, motivated by the rich quantum geometry of topological materials, we identify a set of odd nonlinear acoustoelastic effects adaptable for constructions of topological acoustic diodes. As a concrete realization of such a topological acoustic diode, we propose acoustically driven axion insulators, phases of matter that have been experimentally retrieved recently [52–54]. We demonstrate that the θ vacua of axion insulators not only realize odd acoustic rectifications, central to the operation of acoustic diodes, but also demonstrate odd acoustic SHG. We fully characterize the quantum-geometric nature of this acoustic SHG response of topological electrons driven by the time-dependent external acoustic deformations.

More fundamentally, we uncover the central role of the quantum nonmetricity tensor, reflecting the quantum metric incompatibility of the Hermitian connection over the manifold of cell-periodic Bloch states. This provides a capstone to the set of Riemannian-geometric tensors manifested in quadratic material responses. Beyond retrieving uncharted acoustoelastic phenomenology, we showcase how the odd responses of an axionic topological acoustic diode can be experimentally probed and adapted for topological engineering purposes. Finally, we discuss how the realization of identified odd acoustoelastic effects may impel further pursuits in terms of broader applications of topological materials.

Results.—In the following, we introduce and characterize the nonlinear odd acoustoelastic effects in a topological acoustic diode. We begin by considering frequency components of distortion fields $w_{ij}(\omega) = \frac{\partial u_i(\omega)}{\partial x_j}$, with elastic displacements $x_i \rightarrow x_i + u_i(\omega)$ in spatial coordinates x_i , and frequencies ω under time-dependent deformations $u_i(t) = \int d\omega e^{i\omega t} u_i(\omega)$. Distortions are then implemented by gauging momenta using a generalized Peierls substitution $k_j \rightarrow k_j - w_{ij} \sin(ak_i)/a$ with a the lattice constant [49, 55]. The nonlinear acoustoelastic currents in response to time-dependent distortion fields $w_{kl}(\omega_1)$ and $w_{mn}(\omega_2)$ read

$$J_{ij}(\Omega) = \eta_{ij;kl,mn}(\omega_1, \omega_2) w_{kl}(\omega_1) w_{mn}(\omega_2), \quad (1)$$

with the nonlinear acoustic response function given by $\eta_{ij;kl,mn}(\omega_1, \omega_2)$ and Einstein summation implied over spatial coordinate indices. This results in elastic momentum currents $J_{ij}(\Omega)$ with frequency $\Omega = \omega_1 + \omega_2$, for any pair of input frequencies ω_1, ω_2 . In particular, we focus on odd acoustic SHG ($\omega_1 = \omega_2$), and dc rectified responses ($\Omega = 0$).

In gapped phases, the corresponding nonlinear odd SHG at sub-gap frequencies, and rectification response functions at arbitrary frequencies, which formally includes contributions from all one-loop diagrams [see the Supplemental Material (SM) [56]], are of the form

$$\eta_{ij;kl,mn}^{\text{odd, SHG}}(\omega, \omega) = \int_{\mathbf{k}} \left[\frac{1}{\omega} \alpha_1 + \alpha_2 + \omega \alpha_3 \right], \quad (2)$$

$$\eta_{ij;kl,mn}^{\text{odd, rect}}(\omega, -\omega) = \int_{\mathbf{k}} \left[\delta(\Delta^{ba} - \omega) \alpha_e + \delta(\Delta^{ba} + \omega) \alpha_h \right], \quad (3)$$

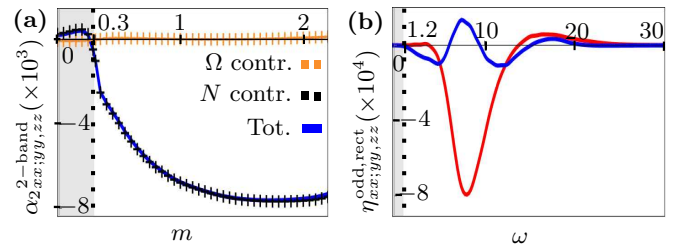


FIG. 2. Nonlinear acoustic responses of an axion insulator diode. (a) Odd second-harmonic response term $\alpha_{2,xx;yy,zz}^{2\text{-band}}$ ($\times 10^3$) against the spin-splitting mass term (m) controlling the band gap. (b) Odd rectification ($\eta_{xx;yy,zz}^{\text{odd,rect}}$) response of a topological acoustic diode vs. frequencies ω . The real (blue) and imaginary (red) parts of the nonlinear acoustic responses reflect distinct dependences on underlying quantum geometries. In the acoustic second-harmonic susceptibility, the nonmetricity tensor (N) contribution dominates the Berry curvature (Ω) term within the total response (Tot.).

with $\int_{\mathbf{k}} \equiv \int_{\text{BZ}} \frac{d^3 \mathbf{k}}{(2\pi)^3}$ a three-dimensional integral over the Brillouin zone (BZ). We present explicit expressions for α_i in Table I. The nonlinear response to dc fields [49] can be retrieved in the zero-frequency limit of the SHG response, reading $\eta^{\text{odd, dc}}(0, 0) = \int_{\mathbf{k}} [-i\tau\alpha_1 + \alpha_2]$, with τ the characteristic scattering time of bulk electrons. In Fig. 1, we showcase the nonlinear phenomenologies of introduced odd acoustic SHG and rectified responses in the specific case of an axion insulator model [57], whose specific formulation is detailed in the End Matter.

We first note that the introduced acoustoelastic responses can be universally decomposed in terms of two-band and three-band contributions, which respectively involve quantum geometric quantities of pairs and triplets of quantum states, see Table I. We find that the odd two-band response in the considered axion insulator model typically dominates over the three-band response contributions: α_1 bears no three-band contribution, and α_2 realizes a two-band contribution that dominates the three-band contribution. However, both terms are comparable for α_3 . The form of three-state contributions is also detailed in the SM [56]. Notably, the numerical acoustic SHG responses show a distinctive change in behavior around a crossover value, $m = 0.3$, see Fig. 2(a). Physically, this occurs when the spin-dependent splitting (m) matches the orbital-dependent splitting (M), and the lower two bands become degenerate at the Γ point of the BZ. The crossover of the orbital- and spin-splitting mass terms introduces a turning point in the quantum geometric terms that underpin the odd nonlinear acoustoelastic responses.

As a central result of this work, we also find that the nonlinear odd acoustoelastic SHG response, α_2 , of the axionic insulator to linearly polarized perturbations is dominated by the nonmetricity (N) contribution, with the geometric Berry curvature (Ω) contribution being negligible, even though the system explicitly breaks time-reversal symmetry (\mathcal{T}), while preserving the inversion

Two-band contribution		Three-band contribution
α_1	$\frac{4i}{3} \sum_{a,b} f_{ba} \left[g_{[(kl,mn)]}^{ba} \partial_{ij} \Delta^{ba} \right]$	\times
α_2	$\sum_{a,b} f_{ba} \left[\frac{\Omega_{ij,(kl,mn)}^{ba} \Delta^{ba}}{\Delta^{ba}} + \frac{32i}{3} N_{[(kl,mn),ij]}^{ba} \right]$	$\frac{2}{3} \sum_{a,b,c} \frac{\text{Re} Q_{ij,(kl,mn)}^{abc}}{\Delta^{ba}} \left(2 + \frac{(\Delta^{ba})^2}{\Delta^{bc} \Delta^{ca}} \right) (f_a \Delta^{bc} + f_b \Delta^{ca} + f_c \Delta^{ab})$
α_3	$\frac{16i}{3} \sum_{a,b} \frac{f_{ba}}{(\Delta^{ba})^2} \left[g_{[(kl,mn)]}^{ba} \partial_{ij} \Delta^{ba} \right]$	$\frac{10i}{3} \sum_{a,b,c} \frac{\text{Im} Q_{ij,(kl,mn)}^{abc}}{(\Delta^{ba})^2} \left(\frac{f_{bc} \Delta^{ca}}{(\Delta^{bc})^2} [2(\Delta^{bc})^2 - \Delta^{bc} \Delta^{ca} - (\Delta^{ca})^2] - \frac{f_{ca} \Delta^{bc}}{(\Delta^{ca})^2} [2(\Delta^{ca})^2 - \Delta^{ca} \Delta^{bc} - (\Delta^{bc})^2] \right)$
α_e	$-\pi \sum_{a,b} f_{ba} \left(\frac{2}{3} \left[g_{[(kl,mn)]}^{ba} \partial_{ij} \Delta^{ba} \right] + \frac{i}{4} \left[\Omega_{kl,mn}^{ba} \partial_{ij} \Delta^{ba} \right] \right)$	\times
α_h	$-\pi \sum_{a,b} f_{ba} \left(\frac{2}{3} \left[g_{[(kl,mn)]}^{ba} \partial_{ij} \Delta^{ba} \right] - \frac{i}{4} \left[\Omega_{kl,mn}^{ba} \partial_{ij} \Delta^{ba} \right] \right)$	\times

TABLE I. Quantum geometric contributions to anomalous nonlinear second-order responses of a topological acoustic diode. Here, (\dots) and $[\dots]$ represent normalized symmetrizations and antisymmetrizations of index pairs. The individual terms are composed of the gauge-invariant geometric tensors and band energy splittings Δ^{ab} , see SM for derivations [56].

symmetry (\mathcal{P}). The nonmetricity tensor is defined as

$$N_{ij,kl,mn}^{ab} = -\tilde{\nabla}_{mn} g_{ij,kl}^{ab}, \quad (4)$$

where $g_{ij,kl}^{ab}$ is the two-state quantum metric tensor in the parameter space of distortions and $\tilde{\nabla}_{mn}$ is the covariant derivative corresponding to the deformation-space Hermitian connection ($\tilde{\Gamma}$) (see SM [56]). Geometrically, the nonmetricity tensor measures the failure of the Hermitian connection to parallel-transport the quantum metric along affinely-parametrized geodesics of the Levi-Civita connection, and thus provides a quantitative measure of how distances and angles vary along momentum-space geodesics. Notably, the nonmetricity averaged over momentum space can be directly extracted from the response of any system modeled by a \mathcal{PT} -symmetric effective two-band Hamiltonian to linearly polarized perturbations, where contributions of all the other terms listed in Table I vanish by definition.

Discussion.—We now discuss and further examine the structure of the odd responses of an axionic topological acoustic diode. First, we note that the retrieved responses are highly dependent on the polarization of the perturbing acoustic waves. Under the decomposition of the responses into terms with distinct frequency scaling [Eqs. (2)–(3)], the coefficients α_1 and α_3 are purely imaginary while α_2 is purely real, and thus linearly polarized elastic perturbations selectively probe α_2 . Notably, the identified nonlinear odd acoustic responses also depend on band torsion, which is captured by the three-state QGT term (see also SM [56]).

We further compare two distinct identified types of nonlinear acoustic phenomena. Unlike the acoustic SHG, the rectification response vanishes below the band gap due to the resonant conditions imposed by the delta functions in Eq. (3). Similarly to dc nonlinear odd viscoelastic effects [49],

the net time-dependent odd responses satisfy sum rules $\eta_{xx;yy,zz} + \eta_{yy;zz,xx} + \eta_{zz;xx,yy} = 0$, and similarly $\eta_{xy;yz,zz} + \eta_{yz;zx,xy} + \eta_{zx;xy,yz} = 0$. Under the Peierls gauge substitution, a related correspondence between the shear and normal deformation stresses holds for the dc and SHG responses: $\eta_{xx;yy,zz} = \eta_{zx;xy,yz} = \eta_{yx;xz,zy}$, but not for the rectification response. This stems from a combination of the internal permutation symmetry and that $\omega_1 = \omega_2$ for dc and SHG, but $\omega_1 \neq \omega_2$ for rectification. Thus, the odd acoustic rectification (SHG) responses have four (two) independent components amongst $\eta_{xx;yy,zz}$, $\eta_{yy;zz,xx}$, $\eta_{zz;xx,yy}$, $\eta_{xy;yz,zx}$, $\eta_{yz;zx,xy}$, and $\eta_{zx;xy,yz}$. As a result, an external control of the topology and quantum geometry of a three-dimensional phase allows one to tune up to four individual characteristic response parameters within an operational rectification mode of a topological acoustic diode.

The four-fold tunability of the odd rectification of a topological acoustic diode opens up a multitude of quantum engineered applications. The two-state and three-state quantum geometries can, for instance, be controlled with external magnetic fields, which determine the effective spin- and orbital-splitting gaps (m/M) [32]. Within the scope of potential applications of the topological acoustic diodes realizing the retrieved odd nonlinear acoustoelastic effects, we envision ultrasound focussing, ultrasonography, switching and logical devices, high-performance acoustic sensors, and noise control [10, 11]. Importantly, the acoustoelastic effects may be studied in material candidates for axion insulators realizing field-theoretic θ vacua, for instance, recently studied topological antiferromagnetic heterostructures based on the chemical compositions of manganese-doped topological insulators, $\text{MnBi}_{2n} \text{Te}_{3n+1}$ [52, 58–60].

Conclusion.—In summary, we uncover a set of nonlinear odd acoustic responses in topological insulators, that

Name	Definition
Off-diagonal Berry conn.	$A_{ij}^{ab} = i \langle a \partial_{ij} b \rangle$
Diagonal Berry conn.	$\mathcal{A}_{ij}^a = i \langle a \partial_{ij} a \rangle$
Two-state QGT	$Q_{ij,kl}^{ab} = A_{ij}^{ab} A_{kl}^{ba}$
Three-state QGT	$Q_{ij,kl,mn}^{abc} = A_{ij}^{ab} A_{kl}^{bc} A_{mn}^{ca}$
Quantum metric	$g_{ij,kl}^{ab} = \text{Re} Q_{ij,kl}^{ab}$
Berry curvature	$\Omega_{ij,kl}^{ab} = -2\text{Im} Q_{ij,kl}^{ab}$
Berry cov. derivative	$\mathcal{D}_{ij} O^{ab} = \partial_{ij} O^{ab} - i[A_{ij} + \mathcal{A}_{ij}, O]^{ab}$
Hermitian conn.	$\tilde{\Gamma}_{ij,kl,mn}^{ba} = A_{ij}^{ab} (\mathcal{D}_{kl} A_{mn})^{ba}$
Christoffel symbol	$\Gamma_{ij,kl,mn}^{ab} = \partial_{(kl} g_{mn)}^{ba} - \frac{1}{2} \partial_{ij} g_{kl,mn}^{ba}$
Torsion	$\mathcal{T}_{ij,kl,mn}^{ab} = 2\tilde{\Gamma}_{ij;[kl,mn]}^{ba}$
Contorsion	$K_{ij,kl,mn}^{ab} = \frac{1}{2} \mathcal{T}_{ij,kl,mn}^{ab} + \mathcal{T}_{(kl,mn),ij}^{ab}$
Nonmetricity	$N_{ij,kl,mn}^{ab} = -\tilde{\nabla}_{mn} g_{ij,kl}^{ab}$
Disformation	$L_{ij,kl,mn}^{ab} = N_{ij,(kl,mn)}^{ab} - \frac{1}{2} N_{kl,mn,ij}^{ab}$

TABLE II. Quantum geometric quantities arising in the nonlinear acoustic response functions. The quantum geometric nonmetricity tensor is central to the odd acoustic second-harmonic responses, beyond the deformation-space QGTs [50, 51], Levi-Civita connection [61–64], and torsion tensor [41, 42, 65] defined above.

includes anomalous acoustoelastic second-harmonic generation and rectified currents. Motivated by the recent material identification of axion insulators as natural candidates for such effects, these unconventional responses hold diverse promises for future applications of such systems as topological acoustic diodes in experimental platforms and related engineered devices.

Acknowledgements.— The authors thank Giandomenico Palumbo and Marco Polini for helpful discussions. A.J. acknowledges funding from the School of Natural Sciences, University of Manchester. W.J.J. acknowledges funding from the Rod Smallwood Studentship at Trinity College, Cambridge. M.M. was funded by an EPSRC ERC underwrite Grant No. EP/X025829/1. R.-J.S. acknowledges funding from an EPSRC ERC underwrite Grant No. EP/X025829/1, and a Royal Society exchange Grant No. IES/R1/221060, as well as Trinity College, Cambridge. This research was supported in part by grant NSF PHY-2309135 to the Kavli Institute for Theoretical Physics (KITP).

END MATTER

Details on the axion insulator models.— In the following, we provide further details on the effective models of axion insulators and the odd acoustic SHG and rectifications studied in the main text. The model four-band Hamiltonian for an axion insulator studied for nonlinear acoustic responses in this work reads [57]

$$\begin{aligned} \mathcal{H}(\mathbf{k}) = & m_0 \tau^z + m \sigma^z + M \tau^z \sigma^z \\ & + v_{2,xy} \tau^x \sigma^z [\sin(k_x) + \sin(k_y)] + v_{2,z} \tau^x \sigma^x \sin(k_z) \\ & + \sum_{i=x,y,z} [t_{1,i} \tau^z \cos(k_i) + t_{\text{PH},i} \cos(k_i) \\ & + t_{2,i} \tau^y \sin(k_i) + v_{1,i} \tau^x \sigma^i \sin(k_i)], \end{aligned} \quad (5)$$

where σ and τ denote spin- and orbital-sector Pauli matrices, Kronecker products are left implicit, and the spin- and orbital-splitting masses are m and M , respectively. The model parameters are set to: $m_0 = -5$, $M = 0.3$, $t_{\text{PH},x} = t_{\text{PH},y} = 0.3$, $t_{\text{PH},z} = 0$, $t_x = 2.3$, $t_y = 2.5$, $t_z = 3$, $t_{2,x} = 0.9$, $t_{2,y} = t_{2,z} = 0$, $v_{1,x} = v_{1,y} = 3.2$, $v_{1,z} = 2.4$, $v_{2,xy} = 1.5$, $v_{2,z} = 0.4$. This model has inversion symmetry (\mathcal{P}), while the splitting masses m and M explicitly break the time-reversal symmetry (\mathcal{T}), consistently with the conventional symmetries of axion insulators.

In this work, m is varied to study the SHG response, while for the rectified response, we fix $m = 1.2$. The Fermi level is set such that the lower (upper) two bands are fully occupied (unoccupied).

Details on quantum geometry with nonmetricity.— We provide a completed table of quantum geometric quantities on the extended Hilbert space, which capture responses up to quadratic order in perturbations. Beyond the torsion (\mathcal{T}) tensor, these involve the momentum-space nonmetricity (N) and disformation (L) tensors. In Table II, all relevant geometric entities are summarized, starting from the definitions of the Berry connections in the bundles of Bloch states $|a\rangle$. In particular, the corresponding geometric tensors capture variations of Bloch states over the parameter space of acoustic distortion fields w_{ij} , which are generated by variations $\partial_{ij} \equiv \delta/\delta w_{ij}$.

[1] V. V. Konotop, J. Yang, and D. A. Zezyulin, Nonlinear waves in \mathcal{PT} -symmetric systems, *Rev. Mod. Phys.* **88**, 035002 (2016).

[2] C. Ortix, Nonlinear Hall Effect with Time-Reversal Symmetry: Theory and Material Realizations, *Adv. Quantum Technol.* **4**, 2100056 (2021).

[3] T. Ideue and Y. Iwasa, Symmetry breaking and nonlinear electric transport in van der Waals nanostructures, *Annu. Rev. Condens. Matter Phys.* **12**, 201 (2021).

[4] Z. Du, H.-Z. Lu, and X. Xie, Nonlinear Hall effects, *Nat. Rev. Phys.* **3**, 744 (2021).

[5] N. Nagaosa and Y. Yanase, Nonreciprocal transport and optical phenomena in quantum materials, *Annu. Rev. Condens. Matter Phys.* **15**, 63 (2024).

[6] S. Shim, M. Mehraeen, J. Sklenar, S. S.-L. Zhang, A. Hoffmann, and N. Mason, Spin-polarized antiferromagnetic metals, *Annu. Rev. Condens. Matter Phys.* **16** (2025).

[7] M. Suárez-Rodríguez, F. De Juan, I. Souza, M. Gobbi, F. Casanova, and L. E. Hueso, Nonlinear transport in non-centrosymmetric systems, *Nat. Mater.* **1** (2025).

[8] Y. Jiang, T. Holder, and B. Yan, Revealing quantum geometry in nonlinear quantum materials, *Reports on Progress in Physics* **88**, 076502 (2025).

[9] R. Boyd, *Nonlinear Optics*, 4th Ed. (Elsevier, Amsterdam, 2019).

[10] B. Liang, B. Yuan, and J.-c. Cheng, Acoustic Diode: Rectification of Acoustic Energy Flux in One-Dimensional Systems, *Phys. Rev. Lett.* **103**, 104301 (2009).

[11] B. Liang, X. Guo, J. Tu, D. Zhang, and J. Cheng, An acoustic rectifier, *Nature Materials* **9**, 989 (2010).

[12] Y. Su, A. V. Balatsky, and S.-Z. Lin, Quantum Nonlinear Acoustic Hall Effect and Inverse Acoustic Faraday Effect in Dirac Insulators, *Phys. Rev. Lett.* **134**, 026304 (2025).

[13] X.-L. Qi, T. L. Hughes, and S.-C. Zhang, Topological field theory of time-reversal invariant insulators, *Phys. Rev. B* **78**, 195424 (2008).

[14] M. Z. Hasan and C. L. Kane, Colloquium: Topological insulators, *Rev. Mod. Phys.* **82**, 3045 (2010).

[15] J. E. Moore, The birth of topological insulators, *Nature* **464**, 194 (2010).

[16] X.-L. Qi and S.-C. Zhang, Topological insulators and superconductors, *Rev. Mod. Phys.* **83**, 1057 (2011).

[17] J. Kruthoff, J. de Boer, J. van Wezel, C. L. Kane, and R. Slager, Topological Classification of Crystalline Insulators through Band Structure Combinatorics, *Phys. Rev. X* **7**, 041069 (2017).

[18] H. C. Po, A. Vishwanath, and H. Watanabe, Symmetry-based indicators of band topology in the 230 space groups, *Nature Communications* **8**, 50 (2017).

[19] B. Bradlyn, L. Elcoro, J. Cano, M. G. Vergniory, Z. Wang, C. Felser, M. I. Aroyo, and B. A. Bernevig, Topological quantum chemistry, *Nature* **547**, 298 (2017).

[20] N. P. Armitage, E. J. Mele, and A. Vishwanath, Weyl and Dirac semimetals in three-dimensional solids, *Rev. Mod. Phys.* **90**, 015001 (2018).

[21] Y. Tokura, K. Yasuda, and A. Tsukazaki, Magnetic topological insulators, *Nat. Rev. Phys.* **1**, 126 (2019).

[22] B. A. Bernevig, C. Felser, and H. Beidenkopf, Progress and prospects in magnetic topological materials, *Nature* **603**, 41 (2022).

[23] D. E. Parker, T. Morimoto, J. Orenstein, and J. E. Moore, Diagrammatic approach to nonlinear optical response with application to Weyl semimetals, *Phys. Rev. B* **99**, 045121 (2019).

[24] Y. Michishita and R. Peters, Effects of renormalization and non-Hermiticity on nonlinear responses in strongly correlated electron systems, *Phys. Rev. B* **103**, 195133 (2021).

[25] Y. Michishita and N. Nagaosa, Dissipation and geometry in nonlinear quantum transports of multiband electronic systems, *Phys. Rev. B* **106**, 125114 (2022).

[26] M. Mehraeen, Quantum Response Theory and Momentum-Space Gravity, *Phys. Rev. Lett.* **135**, 156302 (2025).

[27] I. Sodemann and L. Fu, Quantum Nonlinear Hall Effect Induced by Berry Curvature Dipole in Time-Reversal Invariant Materials, *Phys. Rev. Lett.* **115**, 216806 (2015).

[28] K. Yasuda, A. Tsukazaki, R. Yoshimi, K. S. Takahashi, M. Kawasaki, and Y. Tokura, Large unidirectional magnetoresistance in a magnetic topological insulator, *Phys. Rev. Lett.* **117**, 127202 (2016).

[29] P. He, H. Isobe, D. Zhu, C.-H. Hsu, L. Fu, and H. Yang, Quantum frequency doubling in the topological insulator Bi₂Se₃, *Nat. Commun.* **12**, 698 (2021).

[30] M. Mehraeen and S. S.-L. Zhang, Proximity-induced nonlinear magnetoresistances on topological insulators, *Phys. Rev. B* **109**, 024421 (2024).

[31] A. M. Essin, J. E. Moore, and D. Vanderbilt, Magneto-electric polarizability and axion electrodynamics in crystalline insulators, *Phys. Rev. Lett.* **102**, 146805 (2009).

[32] A. Sekine and K. Nomura, Axion electrodynamics in topological materials, *Journal of Applied Physics* **129**, 141101 (2021).

[33] T. Morimoto and N. Nagaosa, Chiral Anomaly and Giant Magnetochiral Anisotropy in Noncentrosymmetric Weyl Semimetals, *Phys. Rev. Lett.* **117**, 146603 (2016).

[34] O. O. Shvetsov, V. D. Esin, A. V. Timonina, N. N. Kolesnikov, and E. Deviatov, Nonlinear Hall effect in three-dimensional Weyl and Dirac semimetals, *JETP Lett.* **109**, 715 (2019).

[35] S. Dzsaber, X. Yan, M. Taupin, G. Eguchi, A. Prokofiev, T. Shiroka, P. Blaha, O. Rubel, S. E. Grefe, H.-H. Lai, *et al.*, Giant spontaneous Hall effect in a nonmagnetic Weyl-Kondo semimetal, *Proc. Natl. Acad. Sci. U.S.A.* **118**, e2013386118 (2021).

[36] D. Kumar, C.-H. Hsu, R. Sharma, T.-R. Chang, P. Yu, J. Wang, G. Eda, G. Liang, and H. Yang, Room-temperature nonlinear Hall effect and wireless radiofrequency rectification in Weyl semimetal TaIrTe₄, *Nat. Nanotechnol.* **16**, 421 (2021).

[37] Y. Zhang, V. Kalappattil, C. Liu, M. Mehraeen, S. S.-L. Zhang, J. Ding, U. Erugu, Z. Chen, J. Tian, K. Liu, *et al.*, Large magnetoelectric resistance in the topological Dirac semimetal α -Sn, *Sci. Adv.* **8**, eab0052 (2022).

[38] A. Alexandradinata, Quantization of intraband and interband Berry phases in the shift current, *Phys. Rev. B* **110**, 075159 (2024).

[39] F. de Juan, A. G. Grushin, T. Morimoto, and J. E. Moore, Quantized circular photogalvanic effect in Weyl semimetals, *Nature Communications* **8**, 15995 (2017).

[40] J. Ahn, G.-Y. Guo, and N. Nagaosa, Low-frequency divergence and quantum geometry of the bulk photovoltaic effect in topological semimetals, *Phys. Rev. X* **10**, 041041 (2020).

[41] J. Ahn, G.-Y. Guo, N. Nagaosa, and A. Vishwanath, Riemannian geometry of resonant optical responses, *Nature Physics* **18**, 290–295 (2021).

[42] W. J. Jankowski and R.-J. Slager, Quantized Integrated Shift Effect in Multigap Topological Phases, *Phys. Rev. Lett.* **133**, 186601 (2024).

[43] P. Bhalla, K. Das, D. Culcer, and A. Agarwal, Resonant Second-Harmonic Generation as a Probe of Quantum Geometry, *Phys. Rev. Lett.* **129**, 227401 (2022).

[44] A. Bouhon, A. Timmel, and R. Slager, *Quantum geometry beyond projective single bands* (2023), arXiv:2303.02180 [cond-mat.mes-hall].

[45] J. Provost and G. Vallee, Riemannian structure on manifolds of quantum states, *Communications in Mathematical Physics* **76**, 289 (1980).

[46] S. Peotta and P. Törmä, Superfluidity in topologically nontrivial flat bands, *Nature Communications* **6**,

1 (2015).

[47] W. J. Jankowski, A. S. Morris, A. Bouhon, F. N. Ünal, and R.-J. Slager, Optical manifestations and bounds of topological euler class, *Phys. Rev. B* **111**, L081103 (2025).

[48] P. Törmä, Essay: Where Can Quantum Geometry Lead Us?, *Phys. Rev. Lett.* **131**, 240001 (2023).

[49] A. Jain, W. J. Jankowski, M. Mehraeen, and R.-J. Slager, Nonlinear Odd Viscoelastic Effect (2025), [arXiv:2511.22706 \[cond-mat.mes-hall\]](https://arxiv.org/abs/2511.22706).

[50] J. E. Avron, R. Seiler, and P. G. Zograf, Viscosity of Quantum Hall Fluids, *Phys. Rev. Lett.* **75**, 697 (1995).

[51] S. Klevtsov and P. Wiegmann, Geometric Adiabatic Transport in Quantum Hall States, *Phys. Rev. Lett.* **115**, 086801 (2015).

[52] M. M. Otkrov, I. I. Klimovskikh, H. Bentmann, D. Estyunin, A. Zeugner, Z. S. Aliev, S. Gaß, A. U. B. Wolter, A. V. Koroleva, A. M. Shikin, M. Blanco-Rey, M. Hoffmann, I. P. Rusinov, A. Y. Vyazovskaya, S. V. Eremin, Y. M. Koroteev, V. M. Kuznetsov, F. Freyse, J. Sánchez-Barriga, I. R. Amiraslanov, M. B. Babanly, N. T. Mamedov, N. A. Abdullayev, V. N. Zverev, A. Alfonsov, V. Kataev, B. Büchner, E. F. Schwier, S. Kumar, A. Kimura, L. Petaccia, G. Di Santo, R. C. Vidal, S. Schatz, K. Kißner, M. Ünzelmann, C. H. Min, S. Moser, T. R. F. Peixoto, F. Reinert, A. Ernst, P. M. Echenique, A. Isaeva, and E. V. Chulkov, Prediction and observation of an antiferromagnetic topological insulator, *Nature* **576**, 416 (2019).

[53] J.-X. Qiu, C. Tzschaschel, J. Ahn, A. Gao, H. Li, X.-Y. Zhang, B. Ghosh, C. Hu, Y.-X. Wang, Y.-F. Liu, D. Bérubé, T. Dinh, Z. Gong, S.-W. Lien, S.-C. Ho, B. Singh, K. Watanabe, T. Taniguchi, D. C. Bell, H.-Z. Lu, A. Bansil, H. Lin, T.-R. Chang, B. B. Zhou, Q. Ma, A. Vishwanath, N. Ni, and S.-Y. Xu, Axion optical induction of antiferromagnetic order, *Nature Materials* **22**, 583–590 (2023).

[54] J.-X. Qiu, B. Ghosh, J. Schütte-Engel, T. Qian, M. Smith, Y.-T. Yao, J. Ahn, Y.-F. Liu, A. Gao, C. Tzschaschel, H. Li, I. Petrides, D. Bérubé, T. Dinh, T. Huang, O. Liebman, E. M. Been, J. M. Blawat, K. Watanabe, T. Taniguchi, K. C. Fong, H. Lin, P. P. Orth, P. Narang, C. Felsner, T.-R. Chang, R. McDonald, R. J. McQueaney, A. Bansil, I. Martin, N. Ni, Q. Ma, D. J. E. Marsh, A. Vishwanath, and S.-Y. Xu, Observation of the axion quasiparticle in 2D MnBi₂Te₄, *Nature* **641**, 62–69 (2025).

[55] H. Shapourian, T. L. Hughes, and S. Ryu, Viscoelastic response of topological tight-binding models in two and three dimensions, *Phys. Rev. B* **92**, 165131 (2015).

[56] See Supplemental Material (SM), which includes additional Refs. [66–73], for details on the Hermitian connection decomposition (Sec. I), derivation of the odd acoustoelastic response functions (Sec. II), and further details on acoustoelastic response coefficients (Sec. III).

[57] B. J. Wieder and B. A. Bernevig, *The Axion Insulator as a Pump of Fragile Topology* (2018), [arXiv:1810.02373 \[cond-mat.mes-hall\]](https://arxiv.org/abs/1810.02373).

[58] R. S. K. Mong, A. M. Essin, and J. E. Moore, Antiferromagnetic topological insulators, *Phys. Rev. B* **81**, 245209 (2010).

[59] N. H. Jo, L.-L. Wang, R.-J. Slager, J. Yan, Y. Wu, K. Lee, B. Schrunk, A. Vishwanath, and A. Kaminski, Intrinsic axion insulating behavior in antiferromagnetic MnBi₆Te₁₀, *Phys. Rev. B* **102**, 045130 (2020).

[60] A. Gao, Y.-F. Liu, J.-X. Qiu, B. Ghosh, T. V. Trevisan, Y. Onishi, C. Hu, T. Qian, H.-J. Tien, S.-W. Chen, M. Huang, D. Bérubé, H. Li, C. Tzschaschel, T. Dinh, Z. Sun, S.-C. Ho, S.-W. Lien, B. Singh, K. Watanabe, T. Taniguchi, D. C. Bell, H. Lin, T.-R. Chang, C. R. Du, A. Bansil, L. Fu, N. Ni, P. P. Orth, Q. Ma, and S.-Y. Xu, Quantum metric nonlinear Hall effect in a topological antiferromagnetic heterostructure, *Science* **381**, 181–186 (2023).

[61] Y. Gao, S. A. Yang, and Q. Niu, Field Induced Positional Shift of Bloch Electrons and Its Dynamical Implications, *Phys. Rev. Lett.* **112**, 166601 (2014).

[62] B. Hetényi and P. Lévay, Fluctuations, uncertainty relations, and the geometry of quantum state manifolds, *Phys. Rev. A* **108**, 032218 (2023).

[63] M. Mehraeen, Quantum kinetic theory of quadratic responses, *Phys. Rev. B* **110**, 174423 (2024).

[64] A. Jain, W. J. Jankowski, and R.-J. Slager, Anomalous geometric transport signatures of topological Euler class, *Phys. Rev. B* **111**, 235149 (2025).

[65] H.-C. Hsu, J.-S. You, J. Ahn, and G.-Y. Guo, Nonlinear photoconductivities and quantum geometry of chiral multifold fermions, *Phys. Rev. B* **107**, 155434 (2023).

[66] F. W. Hehl, J. D. McCrea, E. W. Mielke, and Y. Ne'eman, Metric-affine gauge theory of gravity: field equations, Noether identities, world spinors, and breaking of dilation invariance, *Phys. Rep.* **258**, 1 (1995).

[67] M. Blau, Lecture Notes on General Relativity, <http://blau.itp.unibe.ch/GRLectureNotes.html>.

[68] E. Blount, Formalisms of band theory, in *Solid state physics*, Vol. 13 (Elsevier, 1962) pp. 305–373.

[69] G. D. Mahan, *Many-particle physics* (Springer Science & Business Media, 2013).

[70] H. Rostami, M. I. Katsnelson, G. Vignale, and M. Polini, Gauge invariance and Ward identities in nonlinear response theory, *Ann. Phys.* **431**, 168523 (2021).

[71] P. Bhalla and H. Rostami, Second harmonic helicity and Faraday rotation in gated single-layer 1T'-WTe₂, *Phys. Rev. B* **105**, 235132 (2022).

[72] P. Bhalla and H. Rostami, Light-induced nonlinear spin Hall current in single-layer WTe₂, *New Journal of Physics* **26**, 023042 (2024).

[73] G. Palumbo, *Weyl Geometry in Weyl Semimetals* (2024), [arXiv:2412.04743 \[cond-mat.mes-hall\]](https://arxiv.org/abs/2412.04743).

SUPPLEMENTAL MATERIAL

Topological Acoustic Diode

Ashwat Jain,^{1,*} Wojciech J. Jankowski,^{2,†} M. Mehraeen,^{1,‡} and Robert-Jan Slager^{1,2,§}

¹*Department of Physics and Astronomy, University of Manchester, Oxford Road, Manchester M13 9PL, UK*

²*TCM Group, Cavendish Laboratory, University of Cambridge, J. J. Thomson Avenue, Cambridge CB3 0HE, UK*

(Dated: January 30, 2026)

CONTENTS

I. Hermitian connection decomposition	2
II. Derivation of the nonlinear response functions	3
III. Nonlinear response coefficients	6
References	8

* ashwat.jain@postgrad.manchester.ac.uk

† wjj25@cam.ac.uk

‡ mandela.mehraeen@manchester.ac.uk

§ robert-jan.slager@manchester.ac.uk

I. HERMITIAN CONNECTION DECOMPOSITION

Here, we briefly review the general decomposition of affine connections on manifolds, see e.g., Refs. [1, 2], for further details. We then apply this to derive useful properties of the Hermitian connection on the manifold of cell-periodic Bloch states. Consider a general connection $\tilde{\nabla}$, which acts on momentum-space rank-2 tensors as

$$\tilde{\nabla}_k \mathcal{O}_{ij} = \partial_k \mathcal{O}_{ij} - \tilde{\Gamma}_{lik} \mathcal{O}_j^l - \tilde{\Gamma}_{ljk} \mathcal{O}_i^l. \quad (1)$$

We use the decomposition $\tilde{\Gamma} = \Gamma_g + C$, where $(\Gamma_g)_{ijk} = \frac{1}{2}(\partial_k g_{ij} + \partial_j g_{ik} - \partial_i g_{jk})$ is a component of the Levi-Civita connection ∇ , which parallel-transports the metric along momentum-space geodesics, $\nabla_i g_{jk} = 0$. The metric-incompatibility of $\tilde{\nabla}$ is captured by the nonmetricity tensor [1–3]

$$N_{ijk} \equiv -\tilde{\nabla}_k g_{ij} = 2C_{(ij)k}, \quad (2)$$

where index (anti-)symmetrizations are normalized as

$$\mathcal{O}_{(i_1 \cdots i_n)j} = \frac{1}{n!} \sum_{\sigma \in S_n} \mathcal{O}_{i_{\sigma(1)} \cdots i_{\sigma(n)} j}, \quad (3a)$$

$$\mathcal{O}_{[i_1 \cdots i_n]j} = \frac{1}{n!} \sum_{\sigma \in S_n} \text{sgn}(\sigma) \mathcal{O}_{i_{\sigma(1)} \cdots i_{\sigma(n)} j}. \quad (3b)$$

S_n denotes the permutation group of n elements and σ a permutation of the set $\{1, \dots, n\}$. In the simplest relevant case ($n = 2$), one has

$$\mathcal{O}_{(ij)} = \frac{\mathcal{O}_{ij} + \mathcal{O}_{ji}}{2}, \quad (4a)$$

$$\mathcal{O}_{[ij]} = \frac{\mathcal{O}_{ij} - \mathcal{O}_{ji}}{2}. \quad (4b)$$

For a scalar field ϕ on the momentum-space manifold, the torsion field is defined as

$$\mathcal{T}_{ijk} \partial^i \phi \equiv [\tilde{\nabla}_j, \tilde{\nabla}_k] \phi = 2\tilde{\Gamma}_{i[jk]} = 2C_{i[jk]}. \quad (5)$$

Using these definitions, it is straightforward to verify that the connection difference tensor field C naturally decomposes into the contorsion K and disformation L tensors as

$$C_{ijk} = K_{ijk} + L_{ijk}, \quad (6)$$

where

$$K_{ijk} = \frac{1}{2}(\mathcal{T}_{ijk} - \mathcal{T}_{jik} - \mathcal{T}_{kij}), \quad (7a)$$

$$L_{ijk} = \frac{1}{2}(N_{ijk} + N_{kij} - N_{jki}). \quad (7b)$$

These inherit the symmetry properties of their constituents

$$K_{ijk} = K_{[ij]k}, \quad (8a)$$

$$L_{ijk} = L_{i(jk)}. \quad (8b)$$

Consider now a Hermitian connection component on the Bloch-state manifold

$$\tilde{\Gamma}_{ijk}^{ba} = A_i^{ab} (\mathcal{D}_j A_k)^{ba} = A_i^{ab} (\partial_j A_k^{ba} - i[\mathcal{A}_j + A_j, A_k]^{ba}), \quad (9)$$

where \mathcal{D}_j is the Berry covariant derivative [4], which takes into account the noncommutativity of the position operator and local

momentum-space operators [5]. The first term on the right-hand side of Eq. (9) is reexpressed as

$$\begin{aligned}
A_i^{ab} \partial_j A_k^{ba} &= \frac{1}{2} \left[A_i^{ab} \partial_j A_k^{ba} + \partial_j (A_i^{ab} A_k^{ba}) - \partial_j A_i^{ab} A_k^{ba} \right] \\
&= \frac{1}{2} \left\{ \partial_j (A_i^{ab} A_k^{ba}) + \partial_k (A_i^{ab} A_j^{ba}) - \partial_i (A_j^{ab} A_k^{ba}) + A_j^{ab} \partial_i A_k^{ba} - A_j^{ba} \partial_i A_k^{ab} \right. \\
&\quad - A_j^{ba} \left[-i(\mathcal{A}_i^a - \mathcal{A}_i^b) A_k^{ab} + i(\mathcal{A}_k^a - \mathcal{A}_k^b) A_i^{ab} - i \sum_c (A_i^{ac} A_k^{cb} - A_k^{ac} A_i^{cb}) \right] \\
&\quad + A_i^{ab} \left[-i(\mathcal{A}_j^a - \mathcal{A}_j^b) A_k^{ba} + i(\mathcal{A}_k^a - \mathcal{A}_k^b) A_j^{ba} + i \sum_c (A_j^{bc} A_k^{ca} - A_k^{bc} A_j^{ca}) \right] \\
&\quad \left. - A_k^{ba} \left[-i(\mathcal{A}_i^a - \mathcal{A}_i^b) A_j^{ab} + i(\mathcal{A}_j^a - \mathcal{A}_j^b) A_i^{ab} - i \sum_c (A_i^{ac} A_j^{cb} - A_j^{ac} A_i^{cb}) \right] \right\}, \tag{10}
\end{aligned}$$

using the relation

$$\partial_i A_j^{ab} - \partial_j A_i^{ab} = i[\mathcal{A}_i + A_i, \mathcal{A}_j + A_j]^{ab}. \tag{11}$$

On reinserting into Eq. (9), and rearranging terms, we arrive at the identity

$$C_{ijk}^{ba} = K_{ijk}^{ba} + \frac{i}{2} (\Gamma_\Omega)_{ijk}^{ba} + i \operatorname{Im}(C_{ijk}^{ba} + \mathcal{T}_{kij}^{ba}), \tag{12}$$

with $(\Gamma_\Omega)_{ijk}^{ba} = \frac{1}{2} (\partial_k \Omega_{ij}^{ba} + \partial_j \Omega_{ik}^{ba} - \partial_i \Omega_{jk}^{ba})$. From this identity, one can readily conclude that the Hilbert-space nonmetricity and disformation tensors are purely imaginary

$$C_{(ijk)}^{ba} = i \operatorname{Im}[C_{(ijk)}^{ba}], \tag{13a}$$

$$N_{ijk}^{ba} = i \operatorname{Im}[N_{ijk}^{ba}], \tag{13b}$$

$$L_{ijk}^{ba} = i \operatorname{Im}[L_{ijk}^{ba}], \tag{13c}$$

and moreover [6, 7],

$$\operatorname{Re}(\tilde{\Gamma}_{ijk}^{ba}) = (\Gamma_g)_{ijk}^{ba} + \operatorname{Re}(K_{ijk}^{ba}). \tag{14}$$

In the main text, we adapt the above decompositions to demonstrate that the imaginary Hilbert-space nonmetricity tensor (N), defined over the parameter space of deformation fields, dominates the odd nonlinear acoustoelastic responses realized in the considered axion insulator models.

II. DERIVATION OF THE NONLINEAR RESPONSE FUNCTIONS

The second-order response function $\eta_{B_0;B_1,B_2}$, for an observable B_0 , upon perturbing fields B_1 and B_2 , with frequencies ω_1 and ω_2 , respectively, can be expressed as the BZ integral of the \mathbf{k} -local response function. In this light, we work with \mathbf{k} -local quantities in this section. For a system with Hamiltonian \mathcal{H} , in the presence of perturbing distortion fields $w_{ij} = \partial u_i / \partial x_j$, a comprehensive evaluation of the nonlinear elastic response tensor $\eta_{ijkl,mn}$ requires considering variations of the Hamiltonian to third order in the distortion field

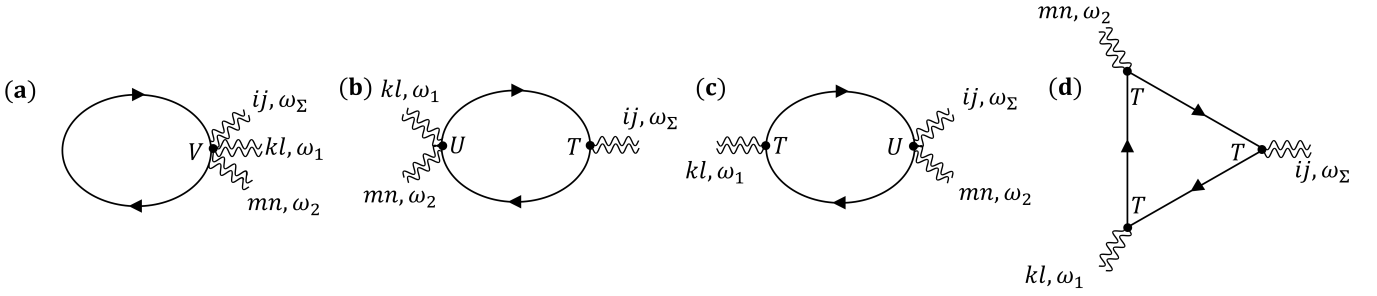
$$T_{ij} = \frac{\delta \mathcal{H}}{\delta w_{ij}}, \tag{15a}$$

$$U_{ij,kl} = \frac{\delta^2 \mathcal{H}}{\delta w_{ij} \delta w_{kl}}, \tag{15b}$$

$$V_{ij,kl,mn} = \frac{\delta^3 \mathcal{H}}{\delta w_{ij} \delta w_{kl} \delta w_{mn}}, \tag{15c}$$

where T is the stress tensor operator and U and V are higher-order counterparts. Generalizing diagrammatic perturbation theory [7–10] to higher-rank tensor distortion field perturbations (see Fig. S1), the nonlinear elasticity tensor can be decomposed into bubble- and triangle-diagram contributions

$$\eta_{ijkl,mn} = \eta_{ijkl,mn}^\circlearrowleft + \eta_{ijkl,mn}^\triangleleft, \tag{16}$$



Supplementary FIG. S1. Diagrammatic structure of the quadratic acoustoelastic tensor $\eta_{ij;kl,mn}$, as a response to tensorial distortions $w_{kl}(\omega_1)$ and $w_{mn}(\omega_2)$. Diagrams (a)-(c) represent the bubble (\circlearrowleft) contributions in Eq. (17), and diagram (d) is the triangle (\triangle) contribution in Eq. (18). Note that each diagram also implicitly denotes a conjugate diagram obtained by swapping (kl, ω_1) with (mn, ω_2) , as required by intrinsic permutation symmetry of the second-order response tensor. Note further that (a) is fully symmetric in the three index pairs.

which take the clean-limit forms [11, 12]

$$\eta_{ij;kl,mn}^{\circlearrowleft}(\omega_1^+, \omega_2^+) = \lim_{\epsilon_1, \epsilon_2 \rightarrow 0} \frac{i(\omega_1^+ + \omega_2^+)}{(i\omega_1^+)(i\omega_2^+)} \sum_{\mathcal{P}} \sum_{a,b,c} \left(V_{ij;kl,mn}^{aa} f_a + f_{ab} \left[\frac{T_{ij}^{ab} U_{kl,mn}^{ba}}{\omega_1^+ + \Delta^{ab}} + \frac{1}{2} \frac{T_{kl}^{ba} U_{ij,mn}^{ab} + T_{mn}^{ba} U_{ij,kl}^{ab}}{\omega_1^+ + \omega_2^+ + \Delta^{ab}} \right] \right), \quad (17)$$

$$\eta_{ij;kl,mn}^{\triangle}(\omega_1^+, \omega_2^+) = \lim_{\epsilon_1, \epsilon_2 \rightarrow 0} \frac{-i(\omega_1^+ + \omega_2^+)}{(i\omega_1^+)(i\omega_2^+)} \sum_{\mathcal{P}} \sum_{a,b,c} \frac{T_{ij}^{ab} T_{kl}^{bc} T_{mn}^{ca}}{\omega_1^+ + \omega_2^+ + \Delta^{ba}} \left(\frac{f_{bc}}{\omega_1^+ + \Delta^{bc}} - \frac{f_{ca}}{\omega_2^+ + \Delta^{ca}} \right). \quad (18)$$

Here, momentum labels are suppressed, $\sum_{\mathcal{P}}$ denotes internal permutation symmetrization between (kl, ω_1) and (mn, ω_2) , band indices are denoted by a, b, c , coordinate indices by i, j, k, l, m, n , matrix elements $\mathcal{O}^{ab} = \langle a | \mathcal{O} | b \rangle$ for any operator \mathcal{O} , $\Delta^{ab} = E^a - E^b$ represents band energy differences, and $f_{ab} = f_a - f_b$ with f_a denoting the Fermi filling factor for band a . Here and hereafter, we represent distortion variations $\delta/\delta w^{ij}$ as δ_{ij} for brevity. The \circlearrowleft term [Eq. (17)] is the contribution from the bubble diagrams [Fig. S1(a)-(c)], while the \triangle term [Eq. (18)] accounts for the triangle diagram [Fig. S1(d)]. In this work, we consider the odd (non-dissipative) part of the response tensor $\eta_{ij;kl,mn}$, which is given by [13]

$$\eta_{ij;kl,mn}^{\text{odd}} = \eta_{ij;kl,mn} - \eta_{(ij;kl,mn)}, \quad (19)$$

where, following Eq. (3), we note that (anti-)symmetrizations are henceforth understood to be over *pairs* of coordinate indices, e.g., $\mathcal{O}_{(ij,kl)} = (\mathcal{O}_{ij,kl} + \mathcal{O}_{kl,ij})/2$.

We also note the following useful relations:

$$T_{ij}^{ab} = \partial_{ij} E^b \delta^{ab} + i \Delta^{ab} A_{ij}^{ab}, \quad (20)$$

$$U_{ij;kl}^{ab} = \partial_{ij} \partial_{kl} E^b \delta^{ab} + i \Delta^{ab} \partial_{ij} A_{kl}^{ab} + i (A_{ij}^{ab} \partial_{kl} \Delta^{ab} + A_{kl}^{ab} \partial_{ij} \Delta^{ab}) - \Delta^{ab} A_{kl}^{ab} (A_{ij}^b - A_{ij}^a) - \sum_c (\Delta^{ac} A_{kl}^{ac} A_{ij}^{cb} + \Delta^{bc} A_{ij}^{ac} A_{ij}^{cb}), \quad (21)$$

$$C_{ij;kl,mn}^{ab} = A_{ij}^{ba} \partial_{kl} A_{mn}^{ab} + i Q_{ij,mn}^{ba} (A_{kl}^b - A_{kl}^a) + T_{ij;kl,mn}^{ab}, \quad (22)$$

$$\mathcal{T}_{ij;kl,mn}^{ba} = -2i \sum_c Q_{ij,[kl,mn]}^{abc}, \quad (23)$$

$$N_{ij;kl,mn}^{ab} = 2C_{(ij;kl,mn)}^{ab}. \quad (24)$$

We can now simplify each of the \circlearrowleft and \triangle contributions to the odd part of the elastic response individually, beginning with the \circlearrowleft contribution. First, we note that the three-photon coupling [Fig. S1(a), i.e., the first term on the right-hand side in Eq. (17)] is fully symmetric (dissipative) and does not contribute to the odd response. Next, we note that Eq. (17) is symmetric under $kl \leftrightarrow mn$, which allows us to expand the internal permutation symmetry explicitly as

$$\eta_{ij;kl,mn}^{\circlearrowleft}(\omega_1^+, \omega_2^+) = - \lim_{\epsilon_1, \epsilon_2 \rightarrow 0} \frac{i}{2} \frac{(\omega_1^+ + \omega_2^+)}{\omega_1^+ \omega_2^+} \sum_{ab} f_{ab} \left(T_{ij}^{ab} U_{kl,mn}^{ba} \left[\frac{1}{\omega_1^+ + \Delta^{ab}} + \frac{1}{\omega_2^+ + \Delta^{ab}} \right] + \frac{T_{kl}^{ba} U_{ij,mn}^{ab} + T_{mn}^{ba} U_{ij,kl}^{ab}}{\omega_1^+ + \omega_2^+ + \Delta^{ab}} \right). \quad (25)$$

Upon further index manipulations, we can write this as

$$\eta_{ij;kl,mn}^{\circlearrowleft}(\omega_1^+, \omega_2^+) = - \lim_{\epsilon_1, \epsilon_2 \rightarrow 0} \frac{i}{2} \frac{(\omega_1^+ + \omega_2^+)}{\omega_1^+ \omega_2^+} \sum_{ab} f_{ab} \left[T_{ij}^{ab} U_{kl,mn}^{ba} \beta_1^{ab} - (T_{kl}^{ab} U_{ij,mn}^{ba} + T_{mn}^{ab} U_{ij,kl}^{ba}) \beta_2^{ab} \right], \quad (26)$$

where $\beta_1^{ab}, \beta_2^{ab}$ are defined as,

$$\beta_1^{ab} = \frac{1}{\omega_1^+ + \Delta^{ab}} + \frac{1}{\omega_2^+ + \Delta^{ab}}, \quad (27)$$

$$\beta_2^{ab} = \frac{1}{\omega_1^+ + \omega_2^+ + \Delta^{ab}}. \quad (28)$$

$$(29)$$

Next, we extract the odd part using Eq. (19), which yields

$$\eta_{ijkl,mn}^{\circ, \text{odd}}(\omega_1^+, \omega_2^+) = -\frac{i}{6} \sum_{ab} f_{ab} \underbrace{\lim_{\epsilon_1, \epsilon_2 \rightarrow 0} \left[\frac{(\omega_1^+ + \omega_2^+)(\beta_1^{ab} + \beta_2^{ab})}{\omega_1^+ \omega_2^+} \right]}_{\gamma^{ab}} \underbrace{\left[2T_{jk}^{ab} U_{kl,mn}^{ba} - T_{mn}^{ab} U_{ij,kl}^{ba} - T_{kl}^{ab} U_{ij,mn}^{ba} \right]}_{\theta_{ijkl,mn}^{ab}}. \quad (30)$$

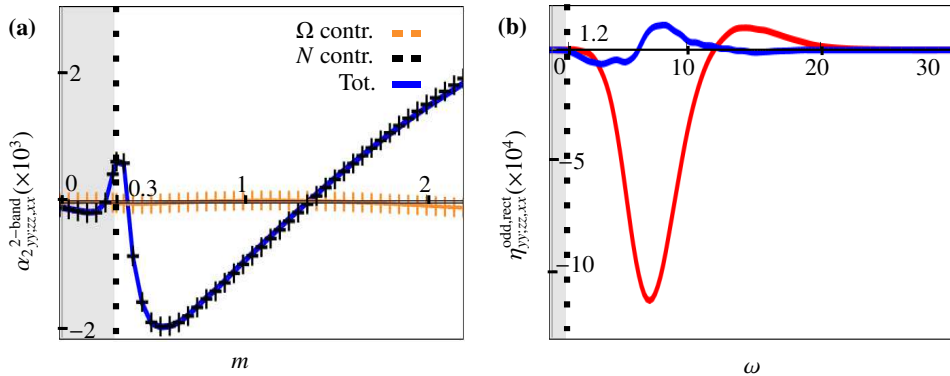
We can now simplify the resonance structure factor γ^{ab} and the matrix element contributions $\theta_{ijkl,mn}^{ab}$ individually. Keeping in mind $\Delta^{ab} \neq 0$ (since we are working with gapped phases), and setting $\epsilon_1 = \epsilon_2$ in order to turn on the perturbing fields at the same rate [10], we can take the relevant limits to write

$$\gamma^{ab} = \frac{2}{\Delta^{ab}} \begin{cases} \frac{1}{i\epsilon} - \frac{4}{\Delta^{ab}}, & \omega_i = 0, \\ \frac{1}{\omega} - \frac{4}{\Delta^{ab}} - \frac{2\omega}{\Delta^{ab}}, & 0 < \frac{\omega_i}{\Delta^{ab}} \ll 1, \\ 0, & \omega_1 + \omega_2 = 0. \end{cases} \quad (31)$$

Importantly, the dc limit must be taken by first setting $\omega_i = 0$, followed by the small ϵ limit, while the non-zero frequency sub-gap acoustic SHG result is obtained by first taking the small ϵ limit, followed by an expansion in ω/Δ^{ab} . Note that the vanishing contribution to the rectification response is calculated at arbitrary frequency, and must be viewed in the sense of a distributional identity, since the Sokhotsi-Plemelj theorem has been used. Notably, the absence of this contribution implies that the total rectification response must arise solely as a Δ contribution.

On the other hand, using Eqs. (20) and (21), and enforcing symmetry under the index permutations, we find that $\theta_{ijkl,mn}^{ab}$ simplifies to

$$\theta_{ijkl,mn}^{ab} = \Delta^{ab} \left\{ 2 \left[2Q_{ij,(kl)}^{ab} \partial_{mn} \Delta^{ab} - Q_{kl,(ij)}^{ab} \partial_{mn} \Delta^{ab} - Q_{mn,(ij)}^{ab} \partial_{kl} \Delta^{ab} \right] + \Delta^{ab} \left[2C_{ij,(kl,mn)}^{ba} - C_{kl,(ij,mn)}^{ba} - C_{mn,(ij,kl)}^{ba} \right] \right. \\ \left. + i \sum_c (\Delta^{ca} + \Delta^{cb}) \left[2Q_{ij,(kl,mn)}^{abc} - Q_{kl,(ij,mn)}^{abc} - Q_{mn,(ij,kl)}^{abc} \right] \right\}. \quad (32)$$



Supplementary FIG. S2. Second independent component (yy; zz, xx) of the nonlinear odd acoustic responses of a model axion insulator [14]. **(a)** The yy; zz, xx component of α_2^2 -band as a function of the spin-splitting mass parameter m . **(b)** The yy; zz, xx rectification response against frequency ω .

Due to the presence of f_{ab} in Eq. (30), the terms proportional to δ^{ab} in $\theta_{ij;kl,mn}^{ab}$ have been abandoned. Furthermore, only certain combinations of terms in the product $\gamma^{ab}\theta_{ij;kl,mn}^{ab}$ survive. In particular, we note that the $1/\epsilon$, $1/\omega$ and ω -linear terms in the expansion will combine non-trivially only with the $a \leftrightarrow b$ odd terms in θ , while the ω -independent terms $4/\Delta^{ab}$ are sensitive only to the even counterparts. This allows us to decompose the responses, as in the main text [Eqs. (1) and (2)], as

$$\alpha_1^\circlearrowleft = \frac{2i}{3} \sum_{ab} f_{ba} \left(g_{(kl,mn)}^{ba} \partial_{ij} \Delta^{ba} - g_{ij,(kl)}^{ba} \partial_{mn} \Delta^{ba} \right), \quad (33)$$

$$\begin{aligned} \alpha_2^\circlearrowleft = & 4 \left[\sum_{ab} f_{ba} \left(\frac{\Omega_{ij,(kl)}^{ba} \partial_{mn} \Delta^{ba}}{\Delta^{ba}} + \frac{4i}{3} (N_{(kl,mn),ij}^{ba} - N_{ij,(kl,mn)}^{ba}) \right) \right. \\ & \left. + \frac{2}{3} \sum_{\substack{a,b,c \\ \neq}} \frac{\text{Re } Q_{ij,(kl,mn)}^{abc}}{\Delta^{ba}} \left(\frac{f_{bc}}{\Delta^{bc}} \left[2(\Delta^{bc})^2 - \Delta^{bc} \Delta^{ca} - (\Delta^{ca})^2 \right] - \frac{f_{ca}}{\Delta^{ca}} \left[2(\Delta^{ca})^2 - \Delta^{ca} \Delta^{bc} - (\Delta^{bc})^2 \right] \right) \right], \end{aligned} \quad (34)$$

$$\begin{aligned} \alpha_3^\circlearrowleft = & \frac{4i}{3} \left[\sum_{ab} \frac{f_{ba}}{\Delta^{ba}} \left(\frac{g_{(kl,mn)}^{ba} \partial_{ij} \Delta^{ba}}{\Delta^{ba}} - \frac{g_{ij,(kl)}^{ba} \partial_{mn} \Delta^{ba}}{\Delta^{ba}} \right) \right. \\ & \left. + \sum_{a,b,c} \frac{\text{Im } Q_{ij,(kl,mn)}^{abc}}{(\Delta^{ba})^2} \left(\frac{f_{bc} \Delta^{ca}}{(\Delta^{bc})^2} \left[-2(\Delta^{bc})^2 + \Delta^{bc} \Delta^{ca} + (\Delta^{ca})^2 \right] - \frac{f_{ca} \Delta^{bc}}{(\Delta^{ca})^2} \left[-2(\Delta^{ca})^2 + \Delta^{ca} \Delta^{bc} + (\Delta^{bc})^2 \right] \right) \right], \end{aligned} \quad (35)$$

where we have split the above expressions into two- and three-band contributions. We have absorbed the torsion contributions into the three-band term using Eq. (23), noting that the torsion and the three-state QGT are fundamentally three-band objects which vanish in two-band systems [7, 15].

We follow an analogous process for the Δ contributions. We take the appropriate sub-gap SHG limit and extract the odd components to obtain

$$\alpha_1^\Delta = 0, \quad (36)$$

$$\alpha_2^\Delta = 3 \sum_{ab} f_{ba} \frac{\Omega_{ij,(kl)}^{ba} \partial_{mn} \Delta^{ba}}{\Delta^{ba}} + 2 \sum_{\substack{a,b,c \\ \neq}} \frac{\text{Re } Q_{ij,kl,mn}^{abc}}{\Delta^{ba}} \left(\frac{f_{bc} \Delta^{ca}}{\Delta^{bc}} [\Delta^{bc} + 3\Delta^{ca}] - \frac{f_{ca} \Delta^{bc}}{\Delta^{ca}} [\Delta^{ca} + 3\Delta^{bc}] \right), \quad (37)$$

$$\alpha_3^\Delta = 2i \left[\sum_{ab} \frac{f_{ba}}{\Delta^{ba}} \left(\frac{g_{(kl,mn)}^{ba} \partial_{ij} \Delta^{ba}}{\Delta^{ba}} - \frac{g_{ij,(kl)}^{ba} \partial_{mn} \Delta^{ba}}{\Delta^{ba}} \right) \right. \quad (38)$$

$$\left. + \sum_{a,b,c} \frac{\text{Im } Q_{ij,(kl,mn)}^{abc}}{(\Delta^{ba})^2} \left(\frac{f_{bc} \Delta^{ca}}{(\Delta^{bc})^2} [2(\Delta^{bc})^2 - \Delta^{bc} \Delta^{ca} - (\Delta^{ca})^2] - \frac{f_{ca} \Delta^{bc}}{(\Delta^{ca})^2} [2(\Delta^{ca})^2 - \Delta^{ca} \Delta^{bc} - (\Delta^{bc})^2] \right) \right]. \quad (39)$$

It should be noted that the α_1 and α_2 components are consistent with the previous findings of Ref. [13]. On combining the bubble and triangle contributions, the total odd response is obtained as $\alpha_i = \alpha_i^\circlearrowleft + \alpha_i^\Delta$.

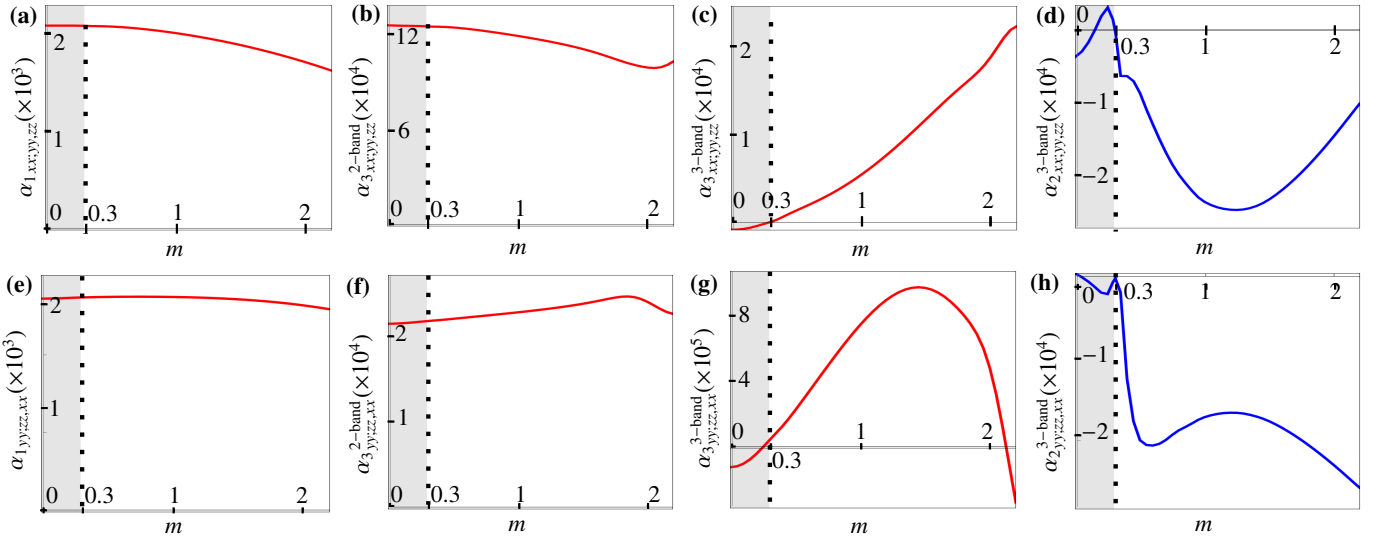
Finally, we obtain the rectification response by setting $\omega_1 = -\omega_2 = \omega$, followed by taking the limit $\epsilon \rightarrow 0$,

$$\begin{aligned} \eta_{ij;kl,mn}^{\text{odd,rect}}(\omega, -\omega, \mathbf{k}) = & \pi \sum_{ab} f_{ab} \left[\frac{1}{3} \left(\delta(\Delta^{ba} - \omega) + \delta(\Delta^{ba} + \omega) \right) \left(g_{(kl,mn)}^{ba} \partial_{ij} \Delta^{ba} - g_{ij,(kl)}^{ba} \partial_{mn} \Delta^{ba} \right) \right. \\ & \left. + \frac{i}{4} \left(\delta(\Delta^{ba} - \omega) - \delta(\Delta^{ba} + \omega) \right) \left(\Omega_{kl,mn}^{ba} \partial_{ij} \Delta^{ba} \right) \right]. \end{aligned} \quad (40)$$

This completes the derivation of Eqs. (1–6) central to the main text after integrating the \mathbf{k} -local quantities over the BZ.

III. NONLINEAR RESPONSE COEFFICIENTS

In this Section, we present the response coefficients complementary to those highlighted in Fig. 2 of the main text. We note that the $yy;zz, xx$ component of $\alpha_2^{\text{2-band}}$, plotted in Fig. S2(a), shows again that the nonmetricity (N) contribution dominates over the Berry curvature (Ω) contribution. We observe a sharp behaviour change at $m = M$, when the lower two bands become degenerate at Γ , similar to Fig. 2(a) in the main text. The behaviour of the rectification response [shown in Fig. S2(b)] is also qualitatively similar to the one demonstrated in the main text, Fig. 2(b). Furthermore, we note that the third coefficient ($zz;xx,yy$) can be inferred from the sum rule: $\eta_{xx;yy,zz} + \eta_{yy;zz,xx} + \eta_{zz;xx,yy} = 0$ [13].



Supplementary FIG. S3. Plots of α_1 , $\alpha_2^{3\text{-band}}$ and α_3 response terms (see Table 1 in the main text). We show both $xx;yy,zz$ and $yy;zz,xx$ response coefficients, complementary to the plots of $\alpha_2^{2\text{-band}}$ presented in the main text (Fig. 2) and in Fig. S2 above.

In Fig. S3, we show the remaining SHG coefficients, as presented in Table I of the main text, for both $xx;yy,zz$ and $yy;zz,xx$ responses. The real parts of the response [$\alpha_2^{3\text{-band}}$, Figs. S3(d) and (h)] are again sensitive to the $m = M$ point, while the $\alpha_3^{3\text{-band}}$ response [Figs. S3(c) and (g)] vanishes near $m = M$.

[1] F. W. Hehl, J. D. McCrea, E. W. Mielke, and Y. Ne’eman, Metric-affine gauge theory of gravity: field equations, Noether identities, world spinors, and breaking of dilation invariance, *Phys. Rep.* **258**, 1 (1995).

[2] M. Blau, Lecture Notes on General Relativity, <http://blau.itp.unibe.ch/GRLectureNotes.html>.

[3] G. Palumbo, *Weyl Geometry in Weyl Semimetals* (2024), arXiv:2412.04743 [cond-mat.mes-hall].

[4] M. Mehraeen, Quantum kinetic theory of quadratic responses, *Phys. Rev. B* **110**, 174423 (2024).

[5] E. Blount, Formalisms of band theory, in *Solid state physics*, Vol. 13 (Elsevier, 1962) pp. 305–373.

[6] H.-C. Hsu, J.-S. You, J. Ahn, and G.-Y. Guo, Nonlinear photoconductivities and quantum geometry of chiral multifold fermions, *Phys. Rev. B* **107**, 155434 (2023).

[7] M. Mehraeen, Quantum Response Theory and Momentum-Space Gravity, *Phys. Rev. Lett.* **135**, 156302 (2025).

[8] G. D. Mahan, *Many-particle physics* (Springer Science & Business Media, 2013).

[9] D. E. Parker, T. Morimoto, J. Orenstein, and J. E. Moore, Diagrammatic approach to nonlinear optical response with application to Weyl semimetals, *Phys. Rev. B* **99**, 045121 (2019).

[10] H. Rostami, M. I. Katsnelson, G. Vignale, and M. Polini, Gauge invariance and Ward identities in nonlinear response theory, *Ann. Phys.* **431**, 168523 (2021).

[11] P. Bhalla and H. Rostami, Second harmonic helicity and Faraday rotation in gated single-layer $1T'$ –WTe₂, *Phys. Rev. B* **105**, 235132 (2022).

[12] P. Bhalla and H. Rostami, Light-induced nonlinear spin Hall current in single-layer WTe2, *New Journal of Physics* **26**, 023042 (2024).

[13] A. Jain, W. J. Jankowski, M. Mehraeen, and R.-J. Slager, Nonlinear Odd Viscoelastic Effect (2025), arXiv:2511.22706 [cond-mat.mes-hall].

[14] B. J. Wieder and B. A. Bernevig, The Axion Insulator as a Pump of Fragile Topology (2018), arXiv:1810.02373 [cond-mat.mes-hall].

[15] J. Ahn, G.-Y. Guo, N. Nagaosa, and A. Vishwanath, Riemannian geometry of resonant optical responses, *Nature Physics* **18**, 290–295 (2021).